Measurement of the expansion of an aluminum plasma heated by *M*-band x rays

T. S. Perry, R. I. Klein, D. R. Bach, K. S. Budil, R. Cauble, H. N. Kornblum, Jr., R. J. Wallace, and R. W. Lee
Lawrence Livermore National Laboratory, P.O. Box 808, Livermore, California 94550
(Received 12 January 1998)

Gold *M*-band x rays produced by irradiating a gold sample with laser light from the Nova laser were used to heat an aluminum foil volumetrically. The hydrodynamic expansion and temperature of the resulting aluminum plasma were measured. The *M*-band source was characterized spatially and temporally, and provided a nearly uniform bulk heating of the sample. This provided an experimental test of hydrodynamic simulations free from the complications of laser-plasma interactions, multiple shocks, or strength of materials. Experiments and simulations of a simple planar expansion and the collision of two parallel foils are presented.
[S1063-651X(98)02809-8]

PACS number(s): 52.50.Jm, 52.70.La, 52.25.Nr

INTRODUCTION

The study of the hydrodynamic motion of materials at high temperatures and pressures is of both scientific and practical interest. Because of their complexity, high temperature plasmas are generally analyzed by multiparameter, multidimensional computer simulation codes that attempt to take into account the large number of physical processes present. Examining the accuracy of these codes requires an experimental design that provides sufficient constraints to allow one physical process to be isolated. This initially requires experiments in which all of the relevant parameters are measured. Later these experiments can be extended to more complicated systems.

We have initiated a series of experiments designed to investigate the hydrodynamic motion of high temperature plasmas produced by volumetric heating of thin metallic foils. The heating source was high energy x rays produced by laser irradiation of thin high-*Z* targets. There have been a number of experiments in which the expansion of thin foils heated in this manner have been measured [1]. However, in those experiments most of the heating energy was deposited at the surface of the foil by low energy x rays. This produced density and temperature gradients in the foil resulting in relatively complicated hydrodynamic motion. Our goal was to design a simpler experiment in which the hydrodynamics could be rigorously investigated. In particular, it was important to avoid any problems arising from laser-plasma interactions or strength of material issues, and to deposit the initial energy in a well-defined manner. These considerations led us to use a short pulse of penetrating x rays (in this case the Au *M* band) to provide the heating for our samples [2].

SOURCE CHARACTERIZATION

To produce the x-ray source we used a 0.3-μm Nova laser [3] beam to irradiate a 1500-Å gold foil deposited on a 3-μm plastic substrate. X rays exiting the rear of the burnthrough target provided the heating source. A 1-ns-long square pulse was focused 1000 μm in front of the target to produce a spot size about 300 μm in diameter. To ensure volumetric heating of the sample foil, a 50-μm-thick plastic filter was placed placed 200 μm from the rear of the target to filter out the low energy part of the spectrum. The 200-μm separation from the gold target prevented the filter from being directly heated by the hot target.

Since hydrodynamic simulations require the specific intensity of the radiation source to initiate the calculations, an absolute source spectrum which could be used in the calculations was required. We used a combination of a crystal spectrometer and a filtered x-ray diode (XRD) array [4]. The XRD array has ten spectral energy channels from 60 eV to 5 keV, and is absolutely calibrated. The spectral response of each XRD channel is determined by filters, x-ray mirrors, and x-ray diodes. However, the energy resolution of the XRD system in the gold *M*-band region of the spectrum is insufficient to give the spectral data required in the simulations. We therefore made spectral measurements of the x rays produced by a gold target in the *M*-band region using a high resolution crystal spectrometer. The high resolution spectrum was then normalized so that the energy emitted over the spectral bandwidth yielded the histogram measured by the XRD.

In contrast with the experiment described in Ref. [2], in which a phase-plate-smoothed laser beam was used, we obtained a much higher conversion to *M*-band radiation with a nonsmoothed beam. Because of the plastic filter, virtually all photon energies below about 2 keV were removed. With 2500 J of incident laser energy we measured 14 J/sr of *M*-band x rays after passing through the 200-μm plastic filter. Correcting for the transmission of the plastic and assuming the production of x rays is isotropic, this implies a 14% conversion from laser light to *M*-band x rays.

Actually, the instantaneous conversion efficiency is even higher. Figure 1 shows the time response of the x-ray production. The intensity of x-ray production falls off nearly linearly with time, even though the laser pulse was square. We interpret this to be due to the breakup of the thin 1500-Å Au target, and the mixing of the Au with the plastic substrate. A thicker gold target would survive longer but would also absorb more of the x rays passing through the target. Low energy x rays produced by laser light interacting with the plastic substrate are filtered out by the separate 50-μm plastic filter shown in Fig. 2. The gold *M*-band spectrum has three broad peaks at approximately 2.0, 2.6, and 3.3 keV; the relative distribution of energy into these peaks is shown in

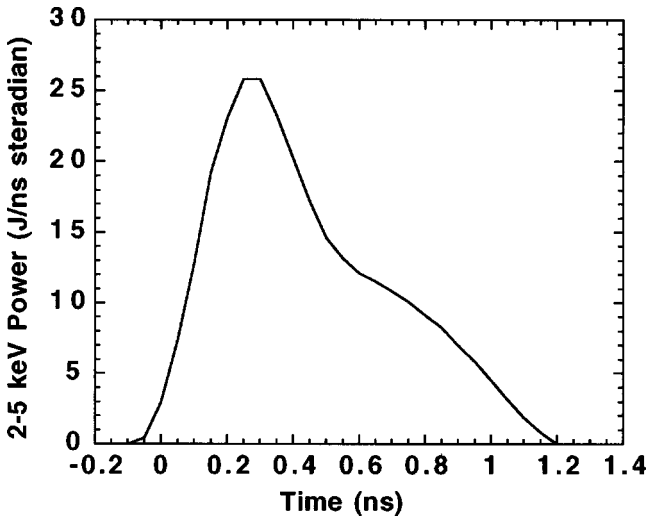

FIG. 1. The measured Au *M*-band power as a function of time produced by a 1-ns square Nova laser pulse shows an approximately linear decay.

the table below. For the hydrodynamic simulation the spectrum was approximated by using only these three spectral energies with the appropriate intensities.

X-ray energy	Relative intensity
2 keV	4.3 J/sr
2.6 keV	8.6 J/sr
3.3 keV	1.1 J/sr

SINGLE-FOIL EXPERIMENT

The experimental arrangement shown in Fig. 2 was used to measure the expansion of both single and double foils. A large x-ray-emitting source was created by using three beams focused so that their spots were lined up side by side. This gave an oval shaped x-ray source area approximately 300 $\times 1000\ \mu m^2$, and ensured one-dimensional motion of the x-ray-driven foils. With the low-energy x-ray contribution removed by the plastic filter, the remaining gold *M*-band radiation heated the 3-μm-thick aluminum foils which were located 1000 μm from the gold x-ray source. The aluminum foils were 800 μm in width, i.e., in the direction transverse to the heating radiation axis, and parallel to the line of sight used by the diagnostics (see Fig. 2).

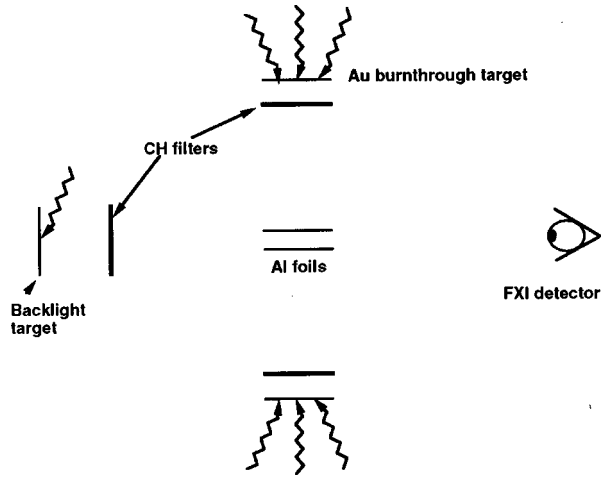

FIG. 2. This is a schematic diagram for the radiatively driven foil experiments. The arrangement shown is for the plasma density measurements. For the single-foil experiment only one burnthrough target was used.

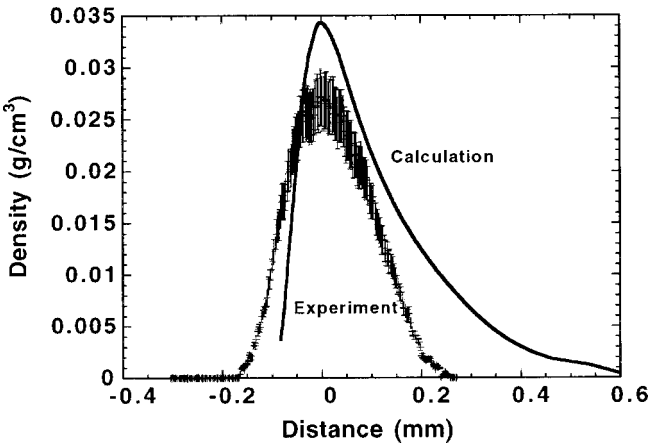

FIG. 3. The measured and calculated density vs position for the single-aluminum-foil experiment at 2.3 ns shows some disagreement.

The expansion of the aluminum foil was observed by using a time-gated x-ray imager. To create a backlight source, a 2000-μm-square piece of tantalum foil was placed at a distance greater than 0.8 cm from the Al foil (see Fig. 2). The Ta foil was illuminated by one of the Nova laser beams at 0.527 μm that had been smoothed by a random phase plate to produce a uniform backlight source typically lasting 2 ns.

Tantalum was chosen because, on the one hand, its *M*-band emission at about 2 keV is at a higher energy than the *K* edge of aluminum at 1.56 keV. Since the aluminum was never ionized beyond the *L* shell in these experiments, the opacity of the aluminum in the 2-keV region was not significantly affected by the Al ionization state. On the other hand, the backlight photon energy should not be much greater than the *K* edge because then the absorption would be small, thus providing poor contrast. To ensure that x rays from the Ta backlight did not affect the hydrodynamics of the aluminum foil, a plastic filter was placed between the foils and the backlight, and the backlight was placed at least eight times farther from the foils than the gold heating source.

Imaging was accomplished by means of a gated x-ray framing camera, the FXI [5], which consists of an array of 10-μm-diameter pinholes and a gated microchannel plate x-ray detector. The FXI diagnostic was designed to produce four spatial images at four different times, providing a total of 16 images with a spatial resolution of 15 μm and a temporal uncertainty in each time of <100 ps. To provide calibration for the density diagnostic procedure, the transmission of a 3-μm-thick strip of aluminum placed over one of the images was used. Each of the remaining three images on each strip imaged the foil from a slightly different angle. This allowed the small spatial variations in backlight intensity to be removed before evaluating the transmission through the foil.

Figure 3 shows the density versus position derived from the single foil experiment. The calculation was the result of a

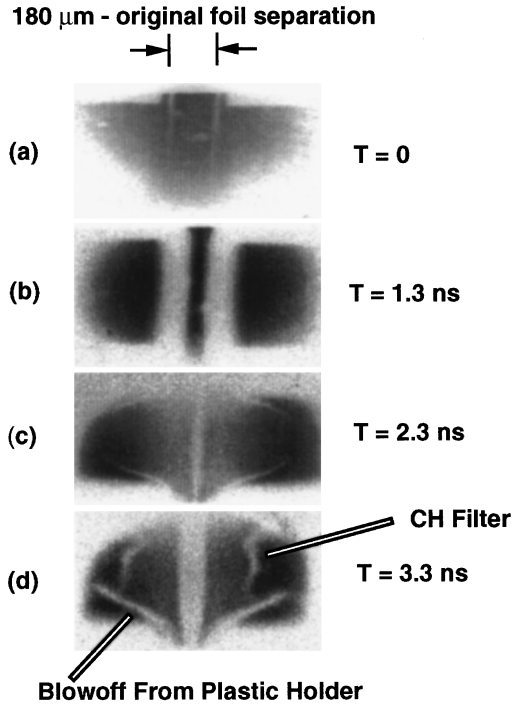

FIG. 4. The raw data for the parallel-aluminum foil-density experiment shows the plasma development as a function of time after the beginning of the laser pulse. Light areas represent areas of high x-ray absorption. (a) The foils before expansion. (b) The two foils have expanded but are not quite making contact with each other. (c) The collision plasma is developing. (d) The collision plasma has fully formed.

one-dimensional radiation hydrodynamic simulation using multigroup implicit Monte Carlo radiation transport and utilizing the x-ray source given in the table above. The experimental curve is almost symmetric, whereas the calculation is not. As the measured density range here is well within the range for an accurate density determination (this is discussed below), there is apparently some difficulty with the symmetry of the simulation, even for this simple geometry. We are currently investigating this discrepancy. At about 5 ns the aluminum foil and the plastic filter, which removed the low energy x rays, began to collide, which limited the duration of the experiment.

PARALLEL-FOIL EXPERIMENT

The overall experimental arrangement for this experiment was similar to that used in the single-foil experiment, except that we studied the motion of two parallel 3-μm-thick aluminum foils, each 800 μm in width, initially separated by 180 μm. Each foil was heated by a separate gold *M*-band source.

Figure 4 shows a set of four transmission images taken at four different times after the initiation of the heating laser pulse. These images are of (a) the foils before expansion, (b) the two foils expanded but not quite making contact with each other, (c) the development of the collision plasma, and finally, (d) the fully formed collision plasma alone. Note that the image at 3.3 ns shows the positions of the CH foils at that time.

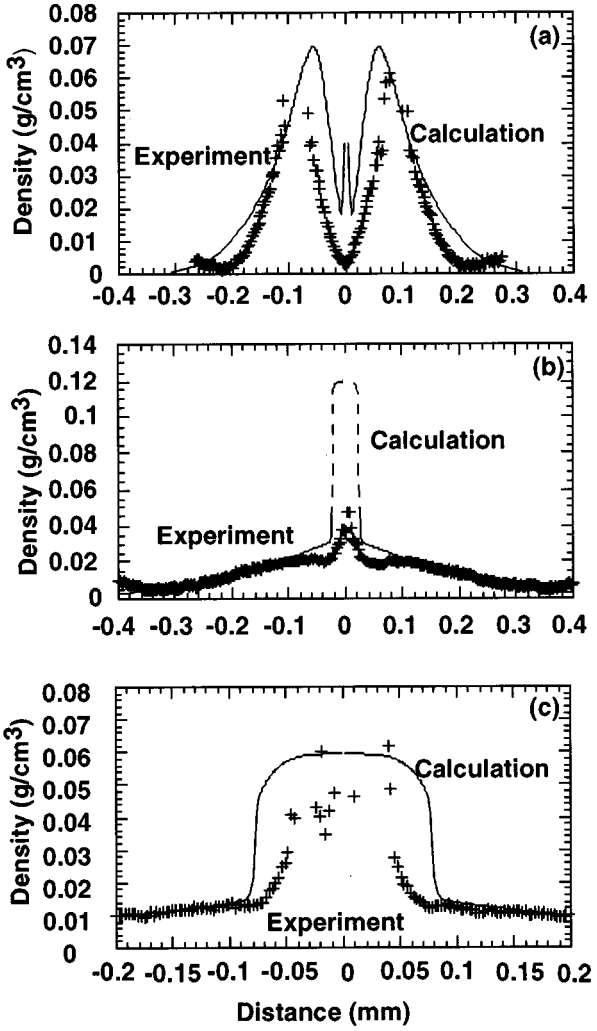

FIG. 5. This figure shows the comparison between the radiation hydrodynamic calculations and the double foil experiments at various times after the beginning of the laser pulse. The dashed line in the upper regions of the calculated curves is used to point out that the experimental data is uncertain here, and cannot be compared with the calculations. (a) The comparison at 1.3 ns. (b) The comparison at 2.3 ns. (c) The comparison at 3.3 ns.

There is a limited range in plasma density that can be measured by this method. The density varies from that of solid aluminum, which occurs before the initiation of the heating laser pulse and results in zero transmission for the backlight x rays, to that of a dilute plasma having little absorption, so that there is effectively no contrast. The upper limit in measurable density therefore depends on the uncertainty in the determination of the detector background signal and noise. The lower limit depends on the accuracy in determination of the backlight spatial distribution across the detector plane and detector noise. For the current experiment, we determined that these limiting factors allowed for densities in the range from 0.005 to 0.05 g/cm^3.

In Fig. 5, we show the density data obtained from the images shown in Fig. 4 together with radiation hydrodynamic simulations. The data were obtained in the same manner as described above in the discussion of the single-foil experiment. The figures show the density distributions obtained at 1.3, 2.3, and 3.3 ns for the double foil experiment.

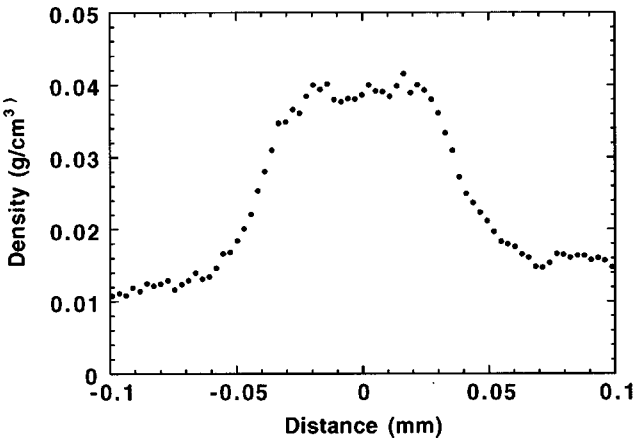

FIG. 6. The measured density of 400-μm-deep Al foils at 3 ns shows a flat-topped density distribution. Note the agreement with the peak of the measured density distribution with that of Fig. 5(c).

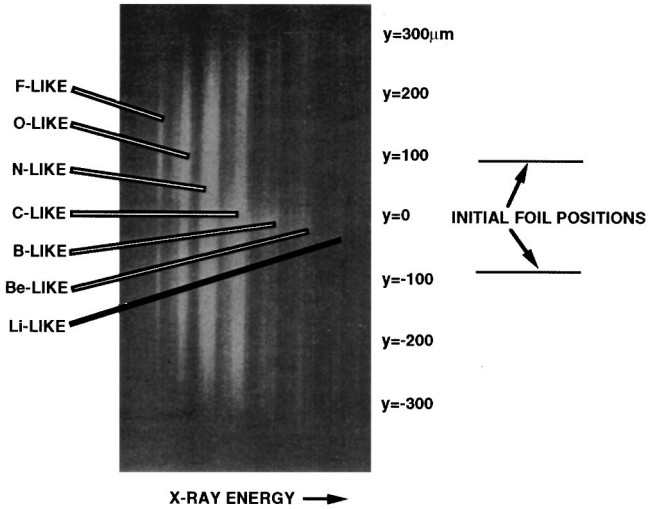

FIG. 7. The spectrometer data at 2 ns from the double-foil experiment shows the variation of plasma temperature with position as seen by the Al 1-2 line absorption.

As seen in Fig. 5(a), which was obtained at 1.3 ns after the beginning of the heating laser pulse, the two parts of the plasma still retain the appearance of the two individual foils. Again, as in the single-foil comparison, there is disagreement with the simulations, particularly in the interpenetration region. The simulation shows the foils expanding slightly faster than in the experiment. Since the drive was measured on a separate shot and varies slightly from shot to shot, this difference in timing is not unexpected.

In Fig. 5(b), which shows the 2.3-ns data, the simulation and experiment are in good agreement in the wings of the density distribution. However, the calculation does not show the well-defined dip which is seen in the experimental curve on either side of the central peak. It should be emphasized that this dip is in the density region where one has confidence in the experiment. The experimental data are not accurate at the peak of the density distribution due to the extremely small transmission.

Figure 5(c) shows the comparison at 3.3 ns. In the central region where the density is high and the transmission low, the measured density data are quite noisy. There was no good background measurement at this time, so background levels were determined by normalizing to the calculations. Nevertheless, the width of the central region and the qualitative shape of the wings could be determined from the measurements. The simulation shows a substantially broader plasma.

In order to obtain more information concerning the late time behavior of the colliding foils, a second experiment with two foils was carried out with the foil width along the axis of the backlight beam reduced to 400 μm, compared to the 800-μm-wide foil used in the earlier shot. Although this increased the two dimensionality of the experiment, it did provide a plasma depth that could be quantified, permitting a reasonable density measurement of the stagnation plasma. A plot from this experiment at 3 ns is shown in Fig. 6. The good agreement between the measured density in the central plateau regions in Figs. 5(c) and 6 is significant. Once again, the simulation does not agree with the data, as the calculated density is 25% too high.

In addition to measuring the density we also determined the temperature of the colliding plasmas as a function of position. This was done by determining the ion balance in the aluminum plasma using a crystal spectrometer to measure the absorption spectrum of the aluminum 1–2 lines through the plasma [6]. The temperature was extracted from the best fit in a series of transmission calculations (OPAL [7]) at the measured density. The densities were sufficiently high that local thermodynamic equilibrium could be assumed in the calculation of the absorption spectra.

For the temperature measurements the tantalum backlight shown in Fig. 2 was replaced by a samarium fiber backlight having a cross section of $25\times100\ \mu m^2$. The primary diagnostic was replaced by a RAP (rubidium hydrogen phthalate) crystal spectrometer. The samarium fiber was illuminated by a tightly focused 200-ps, 700-J, 2ω laser pulse. After passing through the aluminum plasma, these x rays were diffracted by the RAP crystal onto photographic film. The backlight x rays were delayed from the beginning of the heating laser pulse by 2 ns, thus providing a 200-ps spectral snapshot at

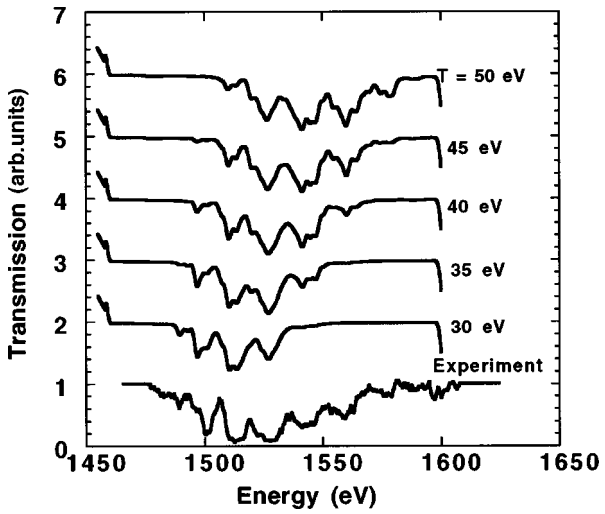

FIG. 8. The calculated x-ray transmission as a function of temperature and comparison with experiment at $\rho=0.027$ g/cm^3 shows a well-defined dependence on the temperature.

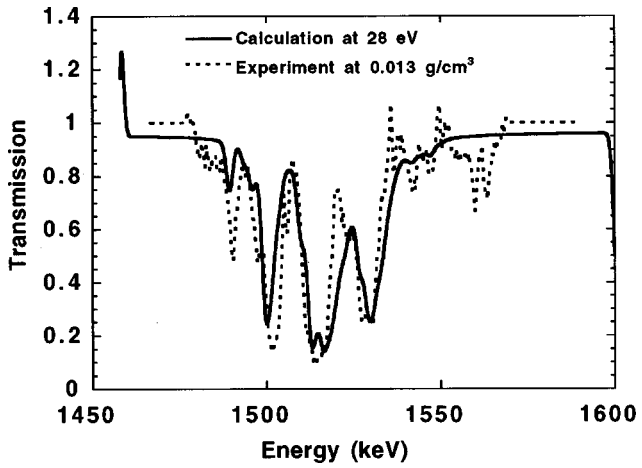

FIG. 9. This is the calculated best fit of the x-ray transmission with experiment. The calculation is at $T=28$ eV and $\rho=0.013$ g/cm^3. The temperature is determined to an accuracy of about 2 eV.

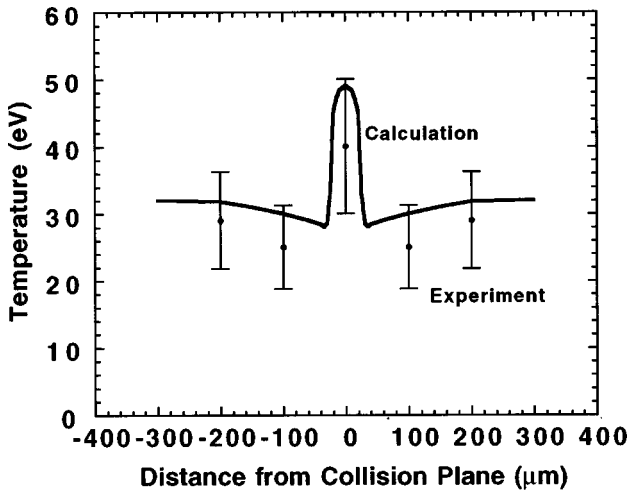

FIG. 10. The measured temperature as a function of position for the parallel-foil experiment shows the estimated error for each data point together with the result of the hydrodynamic simulation calculation.

this time. In contrast to the density measurements, which provided densities at several times on each shot, the spectral measurements required a separate shot for each time point.

In Fig. 7 we show the x-ray transmission film data as a function of x-ray energy for a double-foil experiment, arising from a pair of foils with widths of 200 μm. The smaller width was necessary because there is higher opacity in the bound-bound transitions.

Note that the Li-, Be-, and B-like features of the aluminum 1–2 lines shown in Fig. 7 appear only in the central region between the two foils, indicating a higher temperature in that region of the plasma. A qualitative examination of Fig. 7 also shows that the plasma is fairly symmetric with respect to the midplane between the foils.

A measure of the sensitivity of the x-ray transmission spectrum to temperature is shown in Fig. 8, which contains the results of a series of calculations at different temperatures for a measured density of 0.027 g/cm^3. The measured transmission, which is also shown, contains components of each of the calculated spectra for temperatures from 30 to 50 eV. This indicates that the temperature is a function of position along the spatial direction through which the absorption is measured.

Figure 9 shows a comparison of a best fit OPAL code calculation with the measured transmission. As there is less sensitivity to density than temperature, these data show that the temperature can be determined to an accuracy of 1 or 2 eV if the density is reasonably well known. The experimental-calculational comparisons are not as good here, as they were found to be in the study given in Ref. [6]. This is because the tamping with low-z material used in the former study made the plasma more one dimensional, and prevented noticeable density and temperature gradients.

The results of the temperature diagnostic analysis are shown in Fig. 10, where the temperature as a function of position for the parallel-foil experiment together with the estimated errors due to gradients in the plasma are given. Also shown in the figure are the results of radiation hydrodynamic simulations, which show good agreement with the data.

CONCLUSION

We have developed an experimental procedure for investigating the hydrodynamic behavior of plasmas. Initial conditions were well defined by volumetrically heating each sample with a known flux of penetrating x rays. Density and temperature were both measured, albeit on separate experiments. Temperature and density measurements were sufficiently accurate to make detailed comparisons to radiation hydrodynamic simulations, and demonstrated some limitations of the simulations. These techniques can be used to test plasma radiation hydrodynamic simulation codes rigorously in more complicated geometries.

[1] See. for example, R. Sigel *et al.*, Phys. Rev. A **45**, 3987 (1992); J. Edwards *et al.*, Phys. Rev. Lett. **67**, 3780 (1991); R. A. Bosch *et al.*, Phys. Fluids B **4**, 979 (1992); S. M. Pollaine, R. L. Berger, and C. J. Keane, *ibid.* **4**, 989 (1992).

[2] D. Kania *et al.*, Phys. Rev. A **46**, 7853 (1992).

[3] E. M. Campbell, J. T. Hunt, E. S. Bliss, D. R. Speck, and R. P. Drake, Rev. Sci. Instrum. **57**, 2101 (1986).

[4] H. N. Komblum, R. L. Kauffman, and J. A. Smith, Rev. Sci. Instrum. **57**, 2179 (1986).

[5] K. S. Budil *et al.*, Rev. Sci. Instrum. **67**, 485 (1996).

[6] T. S. Perry *et al.*, Phys. Rev. Lett. **67**, 3784 (1991).

[7] C. A. Iglesias *et al.*, J. Quant. Spectrosc. Radiat. Transf. **51**, 125 (1994).